River network alteration of C-N-P dynamics in a mesoscale agricultural catchment

Antoine Casquin, Sen Gu, Rémi Dupas, Patrice Petitjean, Gérard Gruau, Patrick Durand

Journal Pre-proof

River network alteration of C-N-P dynamics in a mesoscale agricultural catchment

Antoine Casquin, Sen Gu, Rémi Dupas, Patrice Petitjean, Gérard Gruau, Patrick Durand

PII: S0048-9697(20)35080-4

DOI: https://doi.org/10.1016/j.scitotenv.2020.141551

Reference: STOTEN 141551

To appear in: *Science of the Total Environment*

Received date: 10 June 2020

Revised date: 4 August 2020

Accepted date: 5 August 2020

Please cite this article as: A. Casquin, S. Gu, R. Dupas, et al., River network alteration of C-N-P dynamics in a mesoscale agricultural catchment, *Science of the Total Environment* (2020), https://doi.org/10.1016/j.scitotenv.2020.141551

River network alteration of C-N-P dynamics in a mesoscale agricultural catchment

Antoine Casquin [a*], Sen Gu [b, c*], Rémi Dupas [a], Patrice Petitjean [b], Gérard Gruau [b] and Patrick Durand [a]

[a] INRAE, L'institut Agro, UMR 1069 SAS, 35000 Rennes, France

[b] OSUR, Géosciences Rennes, CNRS, UMR 6118, Campus de Beaulieu, 35042 Rennes, France

[c] Institute of Hydrobiology, Chinese Academy of Sciences, Wuhan, 430072 China

[*] Corresponding authors at: antoine.casquin@inrae.fr (Antoine Casquin) and gusen@ihb.ac.cn (Sen Gu)

Abstract

The majority of freshwater ecosystems worldwide suffer from eutrophication, particularly because of agriculture-derived nutrient sources. In the European Union, a discrepancy exists between the scale of regulatory assessment and the size of research catchments. The Water Framework Directive sets water quality objectives at the mesoscale (50-500 km²), a scale at which both hillslope and in-stream processes influence carbon (C), nitrogen (N) and phosphorus (P) dynamics. Conversely, research catchments focus on headwaters to investigate hillslope processes while minimising the influence of river processes on C-N-P dynamics. Because hillslope and river processes have common hydro-climatic drivers, the relative influence of each on C-N-P dynamics is difficult to disentangle at the mesoscale. In the present study, we used repeated synoptic sampling throughout the river network of a 300 km^2 intensively farmed catchment, spatial stochastic modelling and mass balance calculations to analyse this mesoscale conundrum. The main objective was to quantify how river processes altered C-N-P hydrochemical dynamics in different flow, concentration and temperature conditions. Our results show that flow was the main control of alterations of C-N-P dynamics in the river network, while temperature and source concentration had little or no influence. The influence of river processes peaked during low flow, with up to 50% of dissolved organic carbon (DOC) production, up to 100% of nitrate (NO_3) retention and up to 50% of total phosphorus (TP) retention. Despite high percentages of river processes at low flow, their influence on annual loads was low for NO_3 (median of -10%) and DOC (median of +25%) but too variable to draw conclusions for TP. Because of the differing river alteration rates among carbon and nutrients, stoichiometric ratios varied greatly from headwaters to the outlet, especially during the eutrophication-sensitive low-flow season.

Keywords: Carbon; Nitrogen; Phosphorus; In-stream processes; Stochastic modelling; Catchment

1. Introduction

Human activities have impacted water and nutrient cycles considerably in the Anthropocene (Galloway et al., 2003; Steffen et al., 2015; Abbott et al., 2019), with the majority of freshwater and coastal ecosystems worldwide suffering from eutrophication (Le Moal et al., 2018). Eutrophication threatens biodiversity and human water uses such as drinking water, bathing and hydropower production. In western countries, most phosphorus (P) and nitrogen (N) in rivers originates from diffuse agricultural sources (Van Drecht et al., 2003; Dupas et al., 2015). In the European Union, the Water Framework Directive (Water Framework Directive, 2000) sets an objective of good ecological status in all water bodies, and nutrient concentrations are often responsible for not reaching this status. Most water bodies range in size from 50-500 km², which is considered "mesoscale" because of its intermediate size between elementary headwater catchments and large river systems.

In mesoscale catchments, concentration dynamics are influenced by both hillslope and in-stream processes, and their relative effects are difficult to disentangle. Some experimental designs focus specifically on hillslope processes, while others, such as river network studies, focus on in- and near-stream processes.

Research catchments set up in agricultural areas are usually <10 km² (Burns et al., 2019) to capture hillslope processes, but they ignore in-stream processes. Information consists of high-frequency water discharge data and nutrient concentration measurements, sometimes supplemented by soil and groundwater monitoring data. Nutrient dynamics are often interpreted as the result of water pathways in hillslopes that vary according to hydro-climatic variability. River network studies consist either of mechanistic modelling (Garnier et al., 2018) or quantitative estimates of nutrient processing by upscaling results of reach-scale experiments (Wollheim et al., 2008; Mineau et al., 2015). Processing of a nutrient (or carbon (C)) in each segment of a hydrographic network depends on in-stream concentration,

temperature, river stage and water velocity (Mulholland et al., 2008). To calibrate stream-processing rates, multiple tracer injection experiments are necessary; however, these experiments are generally performed in small streams (Tank et al., 2008) and/or during low-flow and steady-state conditions. In-situ measurement of processing coefficients is impractical and uncommon for rivers, although they can have disproportionate impact on downstream nutrient delivery (Ensign and Doyle, 2006; Ye et al., 2017). For rivers with high nutrient concentrations, Aguilera et al. (2013) showed that upscaling coefficients and models derived from reach experiments perform poorly. Calibration of nutrient input into streams relies on correlations between nutrient concentrations and landscape descriptors, such as the percentage of arable fields for N (Wollheim et al., 2008) or percentage of wetlands for C (Wollheim et al., 2015). This approach is not feasible for P, as the correlation between landscape composition and P concentration in headwater catchments is weak (Bol et al., 2018). River network studies often assume that C, N and P are consumed, as most focus on nutrient removal, especially for N. P and C alterations in river networks are discussed less often, and studies that assess C, N and P are even rarer (Maranger et al., 2018).

Instead of studying hillslope and in-stream processes separately, some studies observed an integrated hydrochemical signal in mesoscale and larger catchments. Meybeck and Moatar (2012) and Moatar et al. (2017) developed a segmented method to analyse the concentration-discharge (C-Q) relationship, in which they assumed that in-stream biogeochemical control of the C-Q slope dominated below the median discharge and hillslope hydrological control dominated above the median discharge. Along the same lines, Minaudo et al. (2019) divided C-Q relationships into quickflow and baseflow components. Like in small research catchments, nutrient export patterns at the mesoscale have often been interpreted in terms of spatial distribution of sources vertically and laterally along hillslopes (Dupas et al., 2016; Musolff et al., 2016; Musolff et al., 2017; Abbott et al., 2018; Botter et al., 2019). A positive C-Q slope indicates shallow and/or near-stream sources, while a negative C-Q slope indicates deep and/or upslope sources. These interpretations of C-Q

relationships, however, require caution when two processes influence concentration dynamics in a similar way (Bol et al., 2018; Minaudo et al., 2019). For example, biogeochemical retention within river networks during low flow can easily be confounded with decreasing nutrient delivery caused by a lack of hydrological connectivity with terrestrial nutrient sources.

In this study, we developed a new method to disentangle hillslope from in- and near-stream controls of C-N-P dynamics in a mesoscale catchment. We addressed both apparent retention and apparent production in the river network of C and nutrients without relying on relationships derived from reach-scale experiments. We performed repeated synoptic sampling every two weeks for 18 months, and measured dissolved organic C (DOC), nitrate (NO_3), total P (TP), soluble reactive P (SRP) and chloride (Cl) concentrations in 18 headwater streams and at the outlet of an intensively farmed mesoscale catchment. We then used the headwater catchment data to calibrate a stochastic landscape mixing model to simulate the integrated hillslope nutrient hydrochemical signal of the catchment (expected nutrient concentrations at the outlet assuming no in-stream processes), which we ultimately compared to the hydrochemical signal measured at the outlet. The objectives were to i) quantify the differences observed between modelled and measured nutrient hydrochemical signals at the mesoscale catchment outlet for diverse flow conditions, ii) identify the main control among hydrology, temperature and concentration levels on the observed differences and iii) assess on a seasonal and annual basis the net impact of river network alterations on the export of DOC, NO_3 and TP and possible consequences for downstream ecosystems.

2. Materials and Methods

2.1. Study area

The catchment studied was the 300–km² upper section of the 375–km² Yvel catchment, an agricultural catchment of Strahler order 5 in Brittany, western France (Fig. 1). The Yvel river

is the main tributary of the “Lac au Duc”, a 3–million m^3 recreational and drinking water reservoir downstream of the upper section that has been subjected to cyanobacteria blooms since the 1970s (ODEM, 2012). Hereafter, the article refers to the Yvel catchment exclusively as this 300 km² upper section.

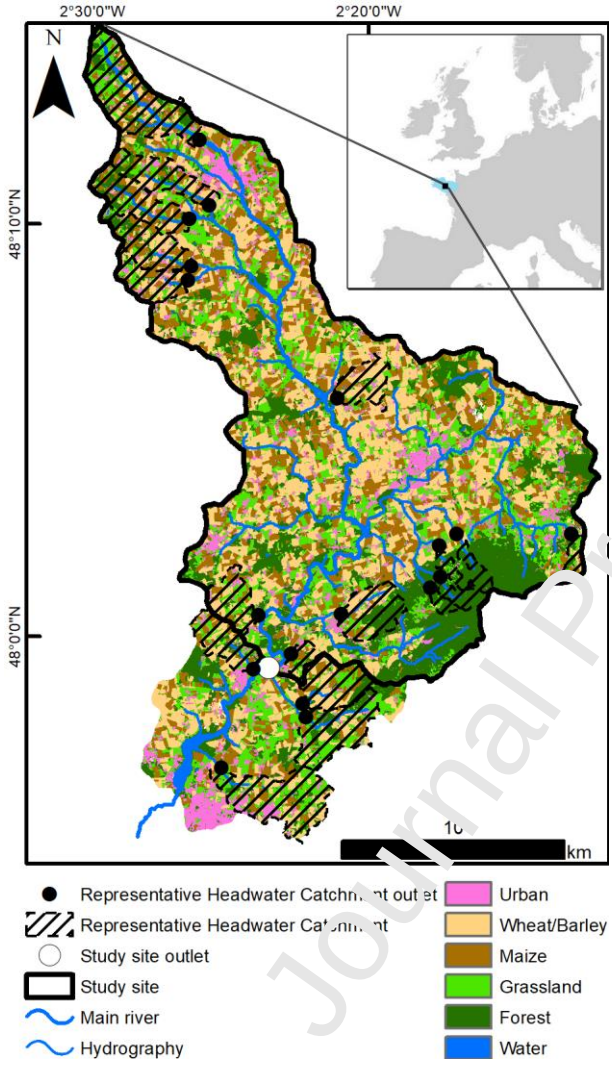

Figure 1. Hydrographic network and land use of the Yvel catchment in 2018. The bold black line outlines the upper section of the Yvel catchment, whose outlet was monitored for water quality and discharge. The dashed areas represent the 18 representative subcatchments monitored, 4 of which lay outside of the upper section of the catchment.

The climate is temperate oceanic, with mean ± standard deviation of annual rainfall, temperature and runoff calculated from 1998-2017 of 777±132 mm, 11.7±0.5°C and 254±143 mm, respectively. The wettest and coldest months (1998-2017) span from November to

March (mean temperature: 7.1°C, mean precipitation: 76 mm.month^{-1}) while the warmest months span from June to September (mean temperature: 17.1°C, mean precipitation: 47 mm.month^{-1}). Almost all precipitation is rain, as freezing temperatures are rare. Elevations range from 33-297 m above sea level. The centre of the catchment is the flattest zone, with most slopes <5%, and long and regular hillslopes. In the north and south, the relief is more uneven, with shorter hillslopes and steeper slopes. The southeast, the forested part of the catchment, has the steepest slopes (5-15%). The bedrock consists of impervious, locally fractured and fissured Brioverian schists, capped by 1-30 m of weathered material. The hydrology is controlled by the dynamics of the shallow water table within the weathered material, as observed in the nearby Kervidy-Naizin research catchment (Molénat et al., 2002). Mean annual discharge at the catchment's outlet is 2,200 L.s^{-1} (19.3 mm.month^{-1}), while mean monthly discharge ranges from 157 L.s^{-1} (1.40 mm.month^{-1}) in August to 5,600 L.s^{-1} (45.16 mm.month^{-1}) in February. The Q90/Q10 ratio (the ratio of the 90th percentile to the 10th percentile of long-term discharge) is 151 (= 6310/41.75). This is consistent with a mostly shallow/reactive hydrological regime, with pronounced low-flow periods and fast and intense floods, as observed in other similar "flashy" catchments in the region.

Soils in the catchment are generally shallow, with 70% of them <70 cm deep (Fig. 1S, Supplementary material). Deeper soils prevail in the north, while thinner soils tend to prevail in the south. Two soil types dominate the catchment: Two soil types dominate the catchment: Luvisols in the north and brown soils (Cambisols) in the rest of the catchment (Fig. 2S, Supplementary material). Shallow undifferentiated soils are found on steep slopes in the southeast. Soils are well drained in plateau and slope domains, but are often hydromorphic in valley bottoms and thus define riparian wetlands (22% of the area of the catchment). Cultivated soils in riparian wetlands are generally tile-drained (Fig. 3S, Supplementary material). Land use was derived from automatic classification of Sentinel 2 satellite images taken during 2018 (Inglada et al., 2017). Arable fields (maize and winter cereals) cover 54% of the catchment (Fig. 1). Grasslands (21%, mostly leys in rotation), forest (18%) and urban

areas (6%) comprise the rest of the catchment. The density of the hedgerow network is 71 $m.ha^{-1}$. The north has a larger percentage of grasslands and more hedgerows than the centre and south. The catchment has a population of ca. 23,100 inhabitants (INSEE, 2015) (6,200 and 5,200 in the two largest towns), which results in a population density of 77 $inhabitants.km^{-2}$. Approximately half of the population is connected to one of the seven wastewater treatment plants (WWTPs), which operate with different technologies (activated sludge, trickling filter, settling ponds) (section 3.3 and Supplementary material section 2), while the other half relies on individual septic tanks. The climate, soil and agricultural properties of the Yvel catchment are similar to the 5 km^2 Kervidy-Naizin research catchment (Fovet et al., 2018), our reference site for catchment research in Brittany (Gascuel-Odoux et al., 2018). With this in mind, the present study can be considered an upscaling exercise from an elementary headwater catchment to a 300 km^2 mesoscale catchment.

2.2. General methodological approach

Our method to estimate the alteration of the signals of NO_3, TP and DOC concentrations by the river network consisted of three main steps (Fig. 2). First, we selected and monitored representative subcatchments to characterise the diversity of headwater hydrochemical signals in the entire catchment. Then, we used a statistical modelling approach, based on landscape composition attributes, to generalise the observations of the monitored subcatchments to all subcatchments in the Yvel catchment. After adding point-source loads from the WWTPs to this signal, we constructed the "source signal" of the Yvel catchment. This source signal had two components (Eq.3, section 2.4.c): diffuse and point-source. The diffuse component was based on the monitored subcatchment signals, which included truly diffuse agricultural sources from fields, small point sources (e.g. leaks from septic tanks or barns) and retention processes within subcatchments. The "classic" point-source component represented chemical loads from the WWTPs. The source signal was an estimate of the hydrochemical signal at the outlet without the in-stream processes in the river network (i.e. those occurring in the water column and hyporheic zone). The hydrochemical signal

observed at the outlet of the entire catchment (i.e. “outlet signal”) was monitored on the same dates as the representative monitored subcatchments. We then estimated in-stream processes as the outlet signal minus the source signal, using stochastic mass balance calculations for the river network, as described in the following subsections.

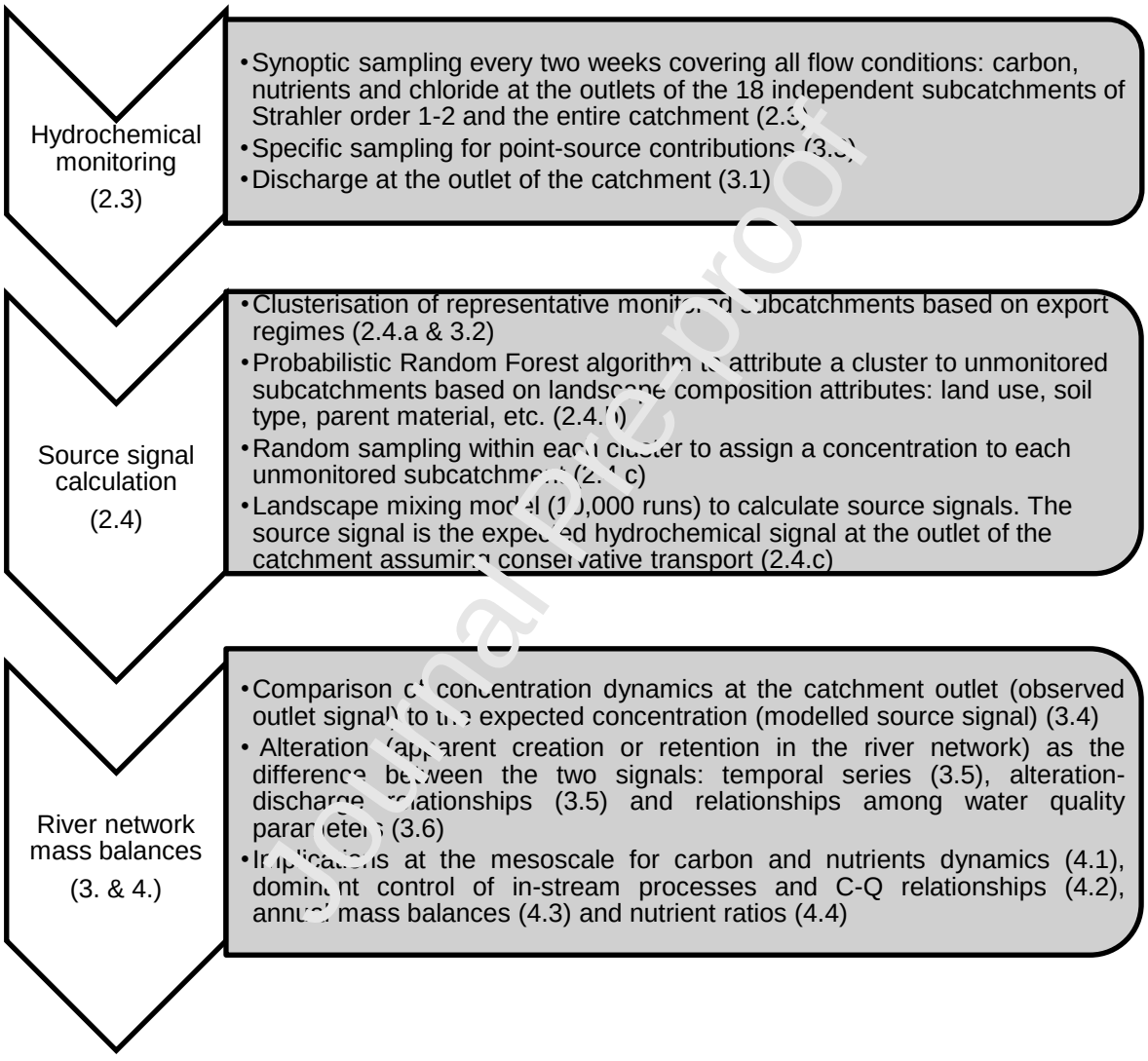

Figure 2. Flowchart of the methodological developed. Numbers in parentheses refer to sections of this article.

2.3. Hydrochemical monitoring

The monitoring strategy consisted of repeated synoptic sampling of the 18 selected monitored subcatchments and the outlet of the entire catchment (Fig. 1). The 18

subcatchments were selected based on their Strahler order (1-2), size (0.8-12.6 km^2), lack of a WWTP, representativeness of the set of subcatchments in the entire catchment and accessibility. Taken together, these 18 subcatchments covered 28% of the Yvel catchment's area (Table S1, Supplementary material).

All 19 monitoring points (monitored subcatchments and outlet of the catchment) were sampled approximately every two weeks from April 2018 to July 2019 (30 dates in total). The seven wastewater treatment plants (WWTP) discharging into the river network were also sampled to evaluate their carbon, nutrient and chloride load. This was done by measuring concentration and discharge immediately upstream and downstream of the plants on two dates: 24 September 2018 and 11 December 2018. Dimensions of the WWTPs ranged from 150-4,700 population equivalent (Table S2, Supplementary material).

All water samples were filtered *in situ* immediately after sampling. Samples were filtered by cellulose acetate filters of 0.45 µm pore size for total dissolved P (TDP) and SRP, and 0.20 µm pore size for DOC, dissolved inorganic C (DIC), Cl and NO_3 analysis. All filters were rinsed in the laboratory with 20 mL of deionised water before use. We also collected an unfiltered water sample to analyse TP. All samples were transported to the laboratory in a cool box and then refrigerated at 4°C until analysis.

P (TP, TDP and SRP) and C (DOC and DIC) were analysed within 48 h of sampling, while anions (NO_3 and Cl) were analysed within one week. Analytical methods described here are for all water samples during the whole 18 months campaign and for WWTP sampling. SRP was determined colorimetrically via reaction with ammonium molybdate (Murphy and Riley, 1962) applied directly to the <0.45 µm filtrates. The same method was used for TDP and TP after digestion of the samples in acidic potassium persulfate. The precision of SRP, TDP and TP measurements was ±4, ±13, ±13 $\mu g.L^{-1}$, respectively. NO_3 and Cl concentrations were analysed by ionic chromatography (Dionex, DX120), with a precision of ±4%. DOC and DIC concentrations were analysed with a total organic analyser (Shimadzu TOC-5050A), with a precision of ±5%, using potassium hydrogen phthalate as the standard solution.

We used NO_3, TP and DOC to characterise the export regimes (section 2.4) and discuss their alterations in the river network throughout this article. We used Cl to assess disconnections of the WWTPs from the river network during the low-flow period. We used alteration of SRP only to interpret that of TP (section 3.6), and TDP and DIC results only to interpret alteration of the nutrient ratio in the river network (section 4.4).

2.4. Source signal calculation

The objective of the stochastic modelling was to generate the source signal. We first need to generate a hydrochemical signal for each unmonitored subcatchment of the Yvel catchment. A stochastic model, calibrated with data from the 18 monitored subcatchments (0.8 – 12.6 km^2) was applied to the 184 unmonitored subcatchments within the catchment, delineated with a 5 m resolution Digital Elevation Model (IGN, 2018). This model uses successively three techniques:

a. Clustering of the 18 monitored subcatchments based on export regime metrics (Hierarchical Clustering on Principal Components - HCPC).
b. Probabilistic classification of the unmonitored subcatchments according to the HCPC clusters, based on landscape composition attributes (Random Forest)
c. Monte-Carlo simulations of the source signal based on the probabilities computed in the previous steps and addition of the point source loads (Landscape mixing model)

a. Headwater clustering

We use FactoMineR package (Lê et al., 2008) v. 1.41 of R software v. 3.5.1 (R Core Team, 2019) to cluster the 18 monitored subcatchments into four clusters using HCPC. The six export regime metrics used in the clustering algorithm were the flow-weighted concentration (FWC) of NO_3, TP and DOC, along with their respective amplitudes of variation. We calculated FWC for each element as follows:

$$FWC = \frac{\sum_d c_d * Q_d}{\sum_d Q_d} \ (Eq. 1)$$

where d is the sampling date, c_d the concentration and Q_d the discharge at the outlet (a proxy of local discharge, which we did not monitor).

We calculated the amplitude of variation of each element as follows:

$$Amplitude = \frac{C90 - C10}{C50} \ (Eq. 2)$$

where C90, C50 and C10 are the 90th, 50th and 10th percentiles of the concentration, respectively.

We calculated FWC and Amplitude for a one-year period (21 June 2018 to 11 June 2019) instead of the entire range of sampling dates, as the latter included April-July twice.

We grouped the 18 subcatchments into 4 clusters because this number of clusters provided a good compromise between cluster homogeneity and the number of subcatchments in each cluster.

b. Classification of unmonitored subcatchments

We classified each of the 184 unmonitored subcatchments into the 4 clusters of the 18 monitored subcatchments. To do this, we calculated nine predictors based on landscape composition: five land-use types (percentage of agricultural, winter crops and summer crops in the subcatchment, percentage of semi-natural areas; percentage of grasslands in the agricultural area), dominant soil and parent material, and percentage of tile drainage and riparian wetlands in the subcatchment. We ran a Random Forest algorithm (Breiman, 2001) using the R package RandomForest v. 4.6-14 (Liaw and Wiener, 2002). We chose eight predictors at each node of the classification tree, performed subsampling with replacement and generated a total of 10,000 trees. Ultimately, for each of the 184 unmonitored subcatchments, the algorithm calculated the probability of belonging to each of the four clusters.

c. Monte-Carlo simulation of the landscape mixing model

To generate the distribution of the diffuse component of the source signals, we performed 10,000 draws of a stochastic landscape mixing model. For each draw, we performed the following steps for each sampling date (n = 30):

1. One cluster is assigned to each unmonitored subcatchment (n = 184) following the probability table obtained through the Random Forest algorithm (Figure 3B)
2. A monitored subcatchment in the selected cluster was randomly assigned to each unmonitored subcatchment according to a uniform distribution (Fig. 3C).
3. The concentration of the diffuse component of each unmonitored subcatchment was set to equal that of the monitored subcatchment assigned (Fig. 3D)

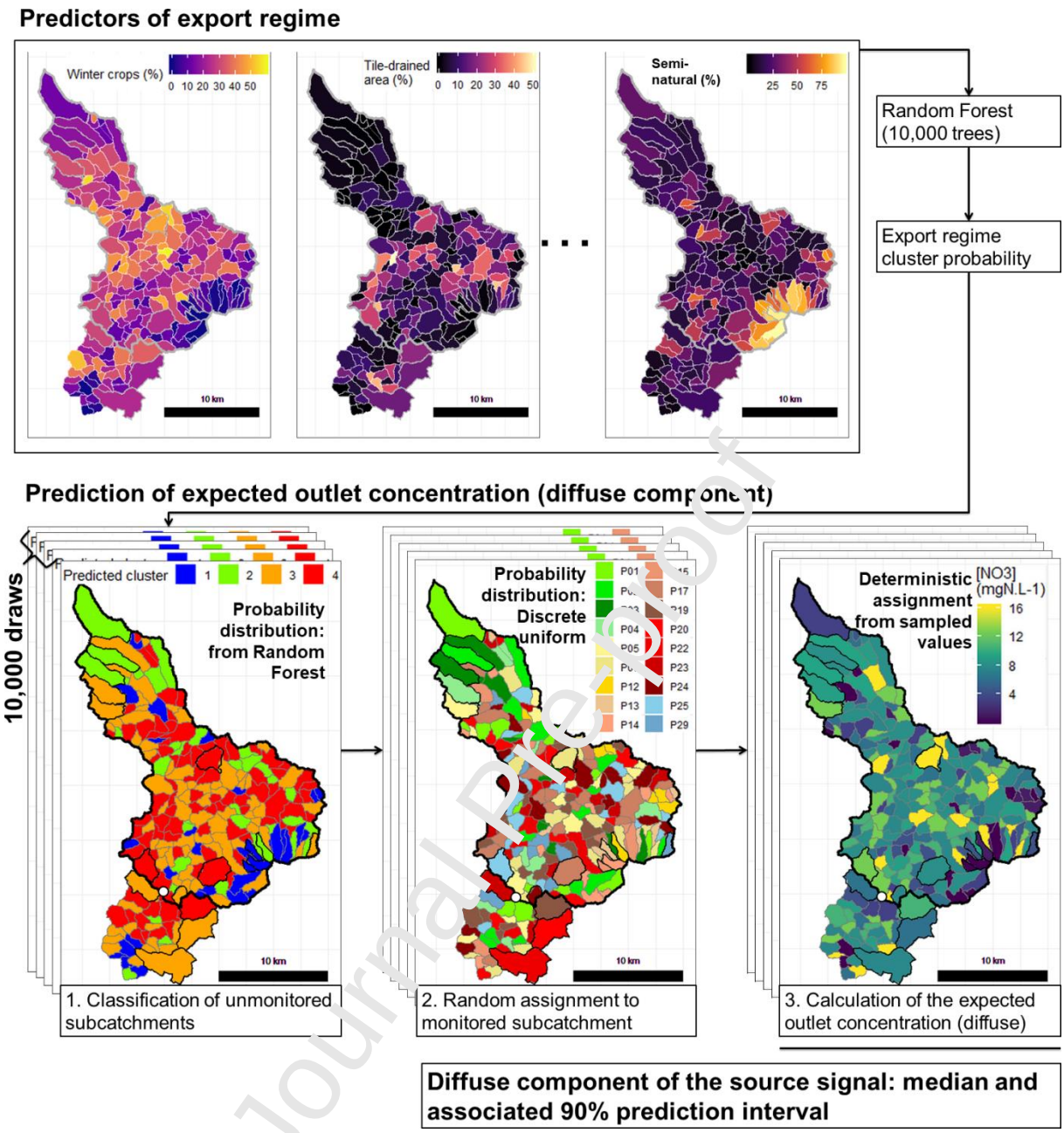

Figure 3. Steps to calculate the diffuse component of the source signal and its associated 90% prediction interval for one element on one date. The example is based on nitrate (NO_3) concentrations measured on 24 April 2018. P01 to P29 in the random assignment map identify the monitored subcatchments. White dots on the maps are the outlet of the catchment. Bold borders outline monitored subcatchments and the entire catchment; light borders outline unmonitored subcatchments.

For each sampling date, this landscape mixing model generated a stochastic diffuse source signal for each subcatchment of the catchment. For each date, the source signal C_d was defined as the sum of its diffuse component and point-source component:

$$C_d = \frac{\sum_i C_{i,d} * A_i}{\sum_i A_i} + k * \frac{b * L_{ps}}{Q_d} (Eq. 3)$$

where $C_{i,d}$ is the expected concentration at the outlet considering conservative transport in the river network, i the number of the subcatchment (n=198; 14 monitored and 184 unmonitored), A_i the area of subcatchment i, L_{ps} the measured point-source load (section 3.3), b a stochastic coefficient (0.8-1.2, different for each draw of the model) used to represent uncertainty in point-source estimates, and k a conversion factor.

Because discharge was available only at the catchment outlet, we assumed the same constant specific discharge throughout the catchment. This assumption is reasonable during stable flow conditions, due to the relatively flat topography, the homogeneous lithology and the relatively small catchment size (Aguilera et al., 2013; Ozuba et al., 2018), but it can lead to unquantified uncertainty during localised storm events. To specify the discharge regime condition during sampling we used the baseflow separation algorithm of Nathan and McMahon (1990) in the Ecohydrology R package of (Fuka et al., 2018). We then calculated a quickflow index based on the quickflow:discharge ratio on each sampling date. The quickflow index was considered "low", "moderate" or "high" when it was <0.33, 0.33-0.67 or >0.67, respectively. On sampling dates during the low-flow period, 1-14 of the monitored subcatchments had dried up depending on the drought severity; they were assigned null concentration and area (A_i - $C_{i,d}$ = 0) when calculating Cd (Eq. 3). We assumed that total point-source load to remain constant throughout the sampling period, which is supported by our observations of NO_3, TP, SRP and Cl (section 3.3). However, we also observed complete disconnect of some WWTPs on the driest dates (discharge <150 $L.s^{-1}$ at the outlet), suggesting that a part of point-source loads on these dry dates did not enter the main river network. We therefore used Cl as a conservative element to estimate the hydrological disconnect during the summer low-flow periods. The proportion of point-source load entering the river network on these dry dates was calculated such that the Cl mass balance remained null at the outlet of the catchment. In order to apply the same methodology in areas affected by saline intrusions, we suggest combining multiple tracers such as pharmaceutical

molecules (carbamazepine, gadolinium) or other organic compounds (caffeine, fluorescent organic matter) (Willams et al. 2013; Richards et al. 2017).

In the mass-balance calculations, alteration signals equalled outlet signals (observed outlet concentrations) minus source signals (modelled expected concentrations). Positive or negative alteration signals represented apparent production or retention, respectively, in the river network. We calculated alteration signals in absolute and relative terms, as a function of both time and discharge. Discharge has been monitored at the catchment outlet since 1968 (gauge J8363110 from DREAL). We used the alteration-discharge (A-Q) relationships for NO_3, TP and DOC to calculate their annual alteration rates (relative mass-balances), as the flow-weighted mean of daily alteration, from 1998-2017.

3. Results

3.1. Hydro-climatic conditions

The water years 2017-2018 and 2018-2019 were normal and dry compared to local mean runoff (253 $mm.y^{-1}$ from 1998-2017), with annual runoff of 238 and 117 $mm.y^{-1}$, respectively. The dates in our sampling campaigns were representative of each of the 10 deciles defined over the 1998-2017 dataset. Of the 30 sampling dates, 13, 13 and 4 had stable, moderately stable and flood-event hydrological conditions (low, moderate and high quickflow, respectively) (Fig. 4). Mean annual temperatures in 2018 and 2019 (11.9 and 11.6°C, respectively) were similar to the long-term mean of 11.7 °C (1998-2017). There was clear seasonality in discharge and temperature, with the high-flow period from December-April and the highest temperature from May-September (Fig. 5).

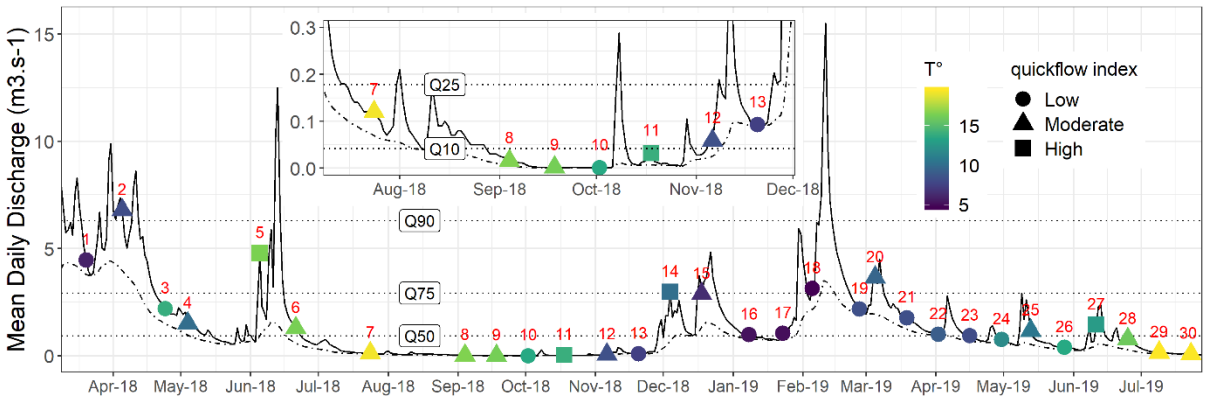

Figure 4. Discharge variations during the study period. The solid line is the mean daily discharge and dot-dash line is the associated baseflow. Horizontal dotted lines indicate 10th, 25th, 75th and 90th percentiles of discharge (Q) from 1998-2017. For each sampling campaign (numbers in red), the shape of the symbol indicates the level of the quickflow index and its colour the mean air temperature of the previous 15 days. The inset shows discharge fluctuations during the low-flow period from July-November 2018.

3.2. Headwater clustering and classification

The four clusters identified by the HCPC clearly differed in export regimes for NO_3, DOC and TP (Fig. 5). Subcatchments in the first cluster (n=3) had low exports of the three elements and large annual amplitudes of NO_3; they corresponded to the forested subcatchments. Subcatchments in the second cluster (n=4) had moderate NO_3 and TP exports but higher DOC export than other clusters; they corresponded to subcatchments with mixed land-use (i.e. annual crops plus grassland and/or forest). Subcatchments in clusters 3 (n=7) and 4 (n=4) had higher NO_3 exports than other clusters. Although most of their land use was arable fields, those in cluster 3 had small amplitudes of TP, while those in cluster 4 had low DOC exports and the highest NO_3 exports of all subcatchments, as well as a larger percentage of tile drainage.

The estimated error rate of the Random Forest algorithm's assignment of an export regime to unmonitored subcatchments was 33%, and the confusion matrix showed that only similar

clusters could be confused (e.g. a cluster 3 monitored subcatchment could be assigned an export regime from cluster 2 or 4 but not from cluster 1). The five most important predictors were the percentage of winter crops and tile-drained land in the subcatchment, percentage of grassland in the agricultural area, dominant soil type and percentage of semi-natural areas in the subcatchment.

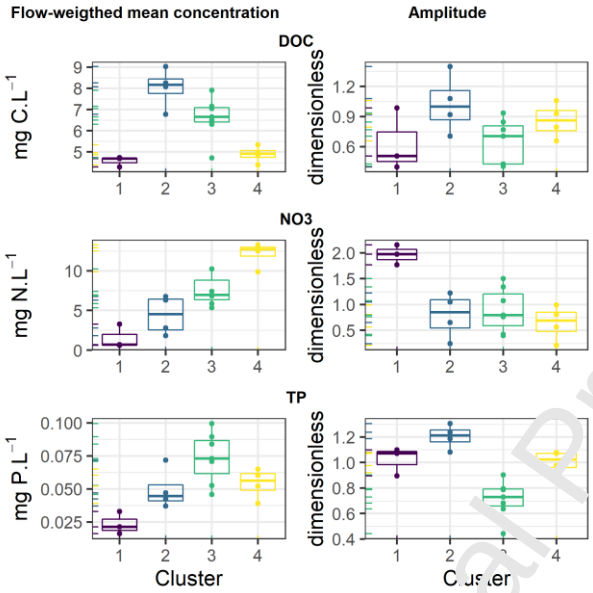

Figure 5. Annual flow-weighted mean concentration and amplitude of DOC, NO_3 and TP in the 18 monitored subcatchments from 21 June 2018 to 11 June 2019 (22 dates), clustered into 4 clusters that differed in export regimes of these elements. Amplitude = (C90-C10)/C50, where C90, C50 and C10 are the 90th, 50th and 10th percentiles of the concentration, respectively.

3.3. Point-source loads

Daily total loads of NO_3, TP, SRP and Cl were similar on both point-source sampling dates (Table 1), despite having completely different flow conditions (Fig. 4). Only DOC loads differed greatly (by one order of magnitude), perhaps due to differences in temperature and flow conditions. Most P leaving the WWTPs was SRP, which represented 82% and 62% of TP load on 24 September and 11 December 2018, respectively.

Table 1. Estimated daily total loads (kg) of NO_3, TP, SRP, DOC and Cl for the two point-source sampling dates

Date	NO_3	TP	SRP	DOC	Cl	Flow condition
24 Sep 2018	53.2	1.97	1.62	18.8	162.8	drought
11 Dec 2018	57.1	2.00	1.25	3.3	168.7	moderate flow

The results indicate that the uncertainty in point-source loads may have been higher than the maximum of 20% assumed in the landscape mixing model (Eq. 3, section 2.4.c), particularly for DOC. Among the WWTPs, two of the smallest contributed disproportionately to the point-source loads of the catchment (Supplementary material).

3.4. Comparing source signal and outlet signal concentrations

Modelled source signals and observed outlet signals had similar concentration medians and ranges for each of the three elements, except during specific events or seasons (Fig. 6).

The modelled source signal for NO_3 ranged from 4.5-9.5 mg $N.L^{-1}$, while the observed outlet signal ranged from 0.5-9.0 mg $N.L^{-1}$. Observed concentrations at the outlet followed a clear seasonal pattern, which the source signal did not, with seasonal maxima during the winter high-flow period and minima during the autumn low-flow period (Fig. 6A). The outlet NO_3 concentration decreased gradually during the summer-autumn recession period but increased sharply during the winter rewetting period. Temporal dynamics of source and outlet signals of NO_3 concentrations matched closely for most of the study period, but not during from July-November 2018 and in July 2019, when concentration was much lower at the outlet (i.e. apparent retention).

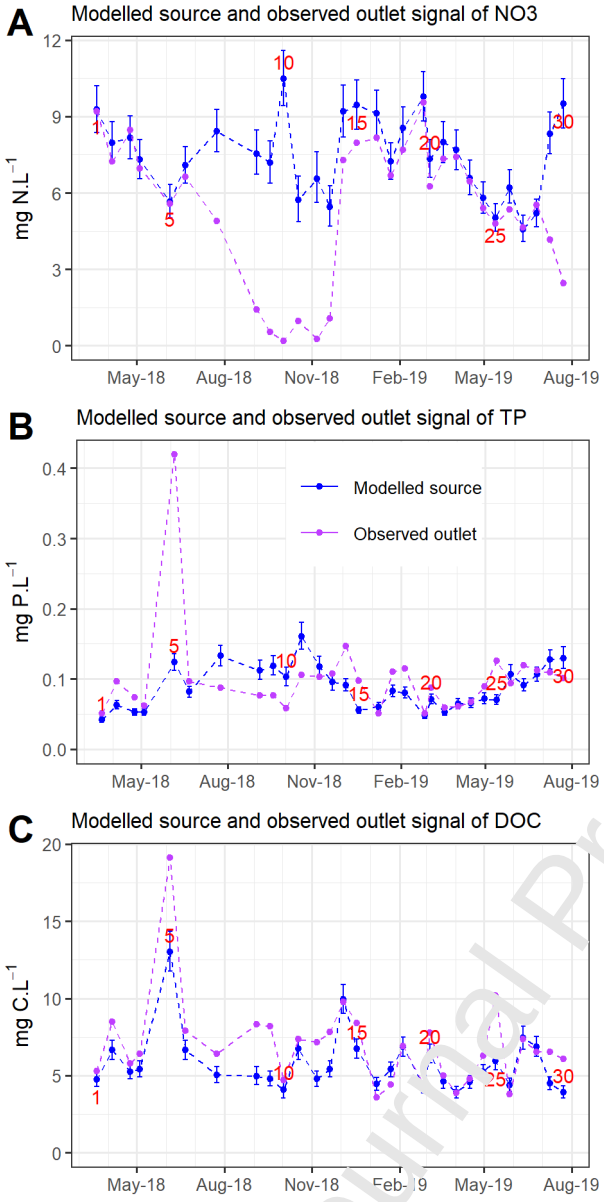

Figure 6. NO_3 (mg $N.L^{-1}$), TP (mg $P.L^{-1}$) and DOC (mg $C.L^{-1}$) concentrations measured at the catchment outlet (outlet signal) on 30 dates and the corresponding modelled expected concentrations (source signal). Error bars on the source signal represent the 90% prediction interval of source concentration obtained from 10,000 draws of the stochastic landscape mixing model (Eq. 3).

The modelled source signal for TP (Fig. 6B) ranged from 0.041-0.151 mg $TP.L^{-1}$, while the observed outlet signal ranged from 0.051-0.420 mg $TP.L^{-1}$. Maximum TP concentrations corresponded to storm events that influenced both the source and outlet signals (sampling campaign no. 5, June 2018). We observed a seasonal pattern in the source signal during the low-flow period, arguably due to the degree of dilution of point-source contributions, but this

seasonal pattern was not clearly visible at the outlet. According to this seasonal pattern in the source signal, TP concentrations peaked in late summer and were lowest in winter. Although source and outlet TP concentrations were similar for most of the year, they differed greatly on specific dates (e.g. campaign no. 5, June 2018) or for entire seasons (e.g. July-October 2018).

The modelled source signal for DOC (Fig. 6C) ranged from 3.6-13.1 mg $C.L^{-1}$, while the observed outlet signal ranged from 3.6-19.1 mg $C.L^{-1}$. Maximum DOC concentrations corresponded to a storm event that influenced both the source and outlet signals (i.e. June 2018). We observed no seasonal pattern in either signal. DOC temporal dynamics at the outlet closely matched those of the source signal, and concentrations were generally similar during winter months while they were higher at the outlet during the rest the year.

3.5. Apparent production and retention by the river network

Alterations estimated between source and outlet signals in the river network revealed moments of apparent production, retention or conservative transport. The “hot moments” of retention or production can correspond to either specific events (e.g. TP apparent production during a flow event, Fig. 7C) or entire periods (e.g. NO_3 apparent retention during the low-flow period, Fig. 7A).

River network alteration of the NO_3 source signal ranged from -98% to +6% (Fig. 7A). In-stream transport was nearly conservative (null alteration lay within 90% prediction interval) on 19 of 30 dates during the study period. We observed net NO_3 retention on the remaining 11 dates, especially during the low-flow period, from September-December 2018, when it exceeded 75% of input. We observed no substantial apparent NO_3 production. The quickflow index did not influence this seasonal retention pattern (e.g. June 2018). There was a linear relationship between NO_3 retention and square-root discharge for discharge <920 $L.s^{-1}$, which corresponds to the median long-term (1998-2017) discharge measured in the catchment (Fig. 7B). Above this discharge threshold, NO_3 transport appeared to be nearly conservative, regardless of temperature. We observed two outliers to this relationship during

the rewetting period of the catchment in December 2018. Applying the alteration-discharge (A-Q) relationship to 10 years (2009-2018) of daily discharge yielded annual apparent NO_3 retention in the river network of 9-14% (Fig. 7B). We calculated annual alteration of NO_3, TP and DOC based on water discharge data only, as neither temperature nor source-signal concentrations (Figs. 4S and 5S, Supplementary material) had an influence.

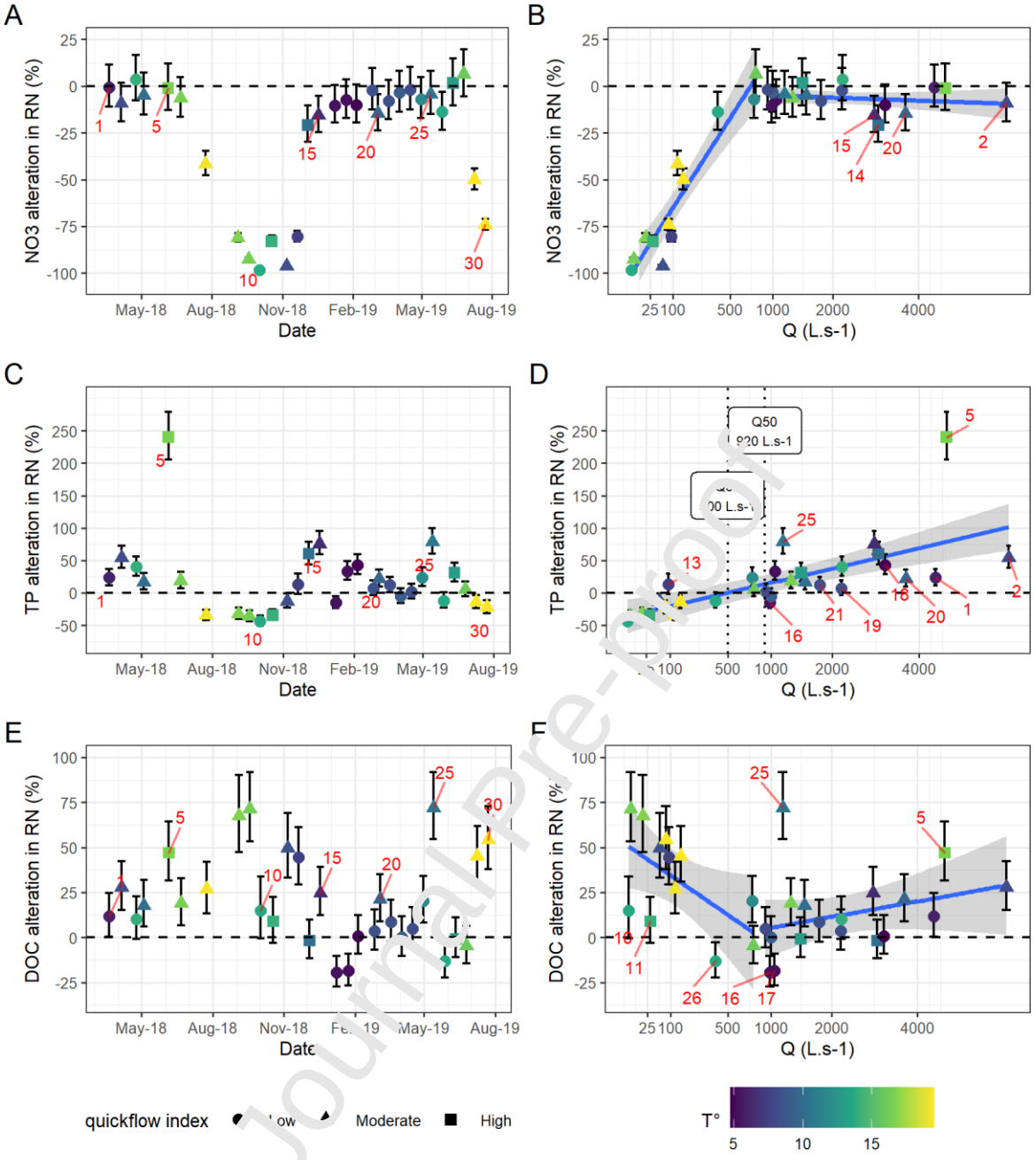

Figure 7. River network (RN) alteration of NO_3, TP and DOC as a function of (A, C and E) sampling date and (B, D and F) square-root-transformed mean daily discharge (Q). Error bars represent 90% prediction interval from 10,000 simulations. Blue lines are linear regressions of the median alteration for Q less than or greater than median Q (Q50). The shape of symbols indicates the quickflow proportion at the time of sampling and their colour the mean air temperature of the previous 15 days.

River network alteration of the TP source signal ranged from -50% to +250% (Fig. 7C). In-stream transport was nearly conservative (null alteration lay within the 90% prediction interval) on only 6 of 30 dates during the study period. Of the remaining dates, 17 showed

apparent production, while 7 showed apparent retention. From September-November 2018, which was dominated by low to very low flow, we observed apparent TP retention even during a small storm event on 18 October. Temporal dynamics of river network retention and production were influenced greatly by flow conditions, with storm events generally resulting in apparent net TP production (e.g. June 2018 and May 2019 storms; campaigns no. 5 and 25, respectively). The linear relationship between apparent TP alteration and square-root discharge had a similar slope below and above median discharge (Fig. 7D). Positive outliers to this relationship corresponded mostly to storm events and rewetting periods (campaign no. 13), while negative ones corresponded to stable hydrological conditions at the end of winter. When discharge was below or above 500 $L.s^{-1}$, we usually observed apparent retention or production, respectively, in the river network. Like for NO_3, we observed no effect of temperature. However, unlike NO_3, we observed no prolonged periods of conservative transport for TP. Assuming that the A-Q relationship during the study period (April 2018 – July 2019) is a constant feature of the studied catchment, the 10 years (2009-2018) of discharge data yielded annual apparent TP production of 42-174%.

River network alteration of the DOC source signal ranged from -19% to +72% (Fig. 7E). In-stream transport was nearly conservative on 11 of 30 dates during the study period. Of the remaining dates, 16 showed apparent production, while only 3 showed apparent DOC retention. A clear seasonal DOC production signal was observed from June-November 2018 (Fig. 7E), with maximum apparent production in September followed by a sharp decrease in October on the two dates when the catchment was the driest (campaigns no. 10 and 11). Two linear relationships between apparent DOC production and square-root discharge had different slopes below and above median discharge (Fig. 7F). The main outlier to this relationship corresponded to a small storm event in May 2019 (campaign no. 25). When discharge was low, we always observed apparent production except during the driest period, while for discharge close to median discharge, transport was often conservative. Like for NO_3 and TP, we observed no direct effect of temperature. We observed three types of outliers,

which corresponded to storm events (like for TP), the driest dates (campaigns no. 10 and 11) or stable high flow in winter (campaigns no. 16 and 17). Applying the A-Q relationship to the 10 years (2009-2018) of daily discharge data, annual apparent DOC production ranged from 16-49%.

3.6. Relationships among water quality parameters

As SRP is not the dominant form of P in streams and rivers, it was not included in the clustering metrics. Nevertheless, we used the same clusters and method to generate the source signal of SRP (Fig. 6S, Supplementary material) and relate it to TP alteration. We hypothesised that SRP has a higher apparent retention rate than TP, which was confirmed by a strong linear relationship between SRP and TP alterations (Fig. 8A) by the river network (slope = 1.77, R^2 = 0.78). The x-axis intercept of the relationship (i.e. conservative TP transport) corresponded to apparent SRP retention of 27%, while the y-intercept of the relationship (i.e. conservative SRP transport) corresponded to apparent TP production of 48%. This implies that the conservative TP transport and some of the apparent TP production may correspond to retention of SRP in the river network, which suggests transformation of SRP into non-reactive P in the river network. Whereas TP was retained on only 6 of 30 dates, SRP was retained on 18 dates. Although both TP and DOC were altered at low flow (Fig. 7D and 7E), there was no relationship between TP retention and DOC production (results not shown). Similarly, no clear relationship emerged between NO_3 retention and DOC production (Fig. 8B), except for a strong NO_3 retention episode during summer/autumn 2018, which corresponded to a period of DOC production. This weak relationship was due to outliers in the DOC A-Q relationship and because apparent DOC production occurred during storm events but not apparent NO_3 retention.

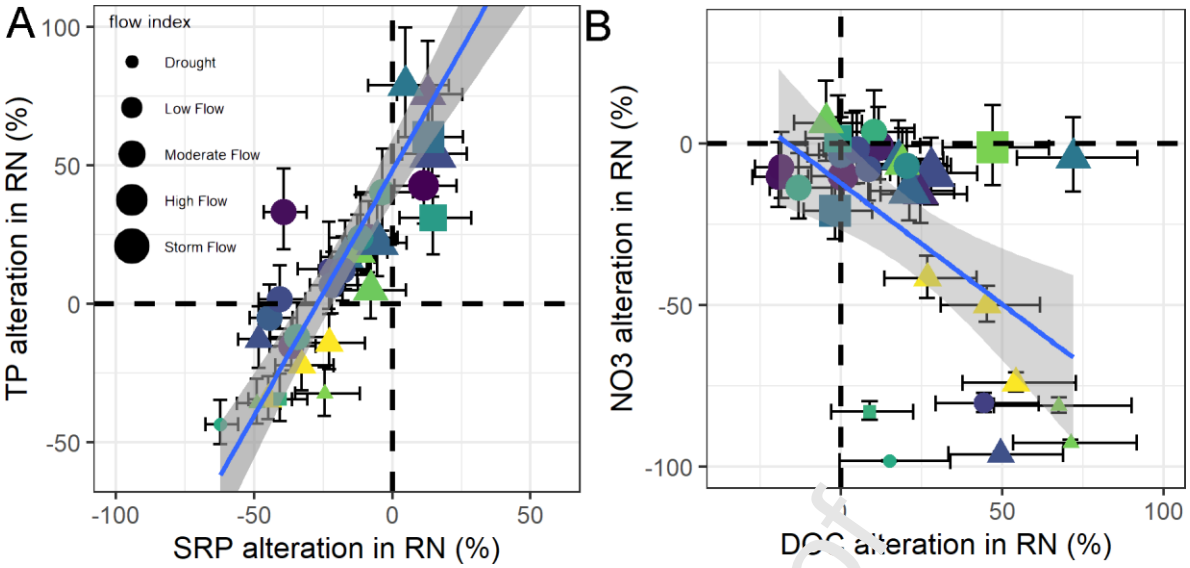

Figure 8. River network (RN) alteration of (A) TP as a function of SRP alteration and (B) NO_3 alteration as a function of DOC alteration. Error bars represent 90% prediction interval from 10,000 simulations. In A, the June 2018 storm value is not shown to keep the scale small but was included in the regression. Blue lines in A and B shows the linear regression between median alterations. The shape of symbols indicates the quickflow proportion at the time of sampling, their colour the mean air temperature of the previous 15 days and their size a flow index. The flow index, calculated according to discharge at the outlet and percentiles of long-term discharge, was classified as "drought" for Q≤Q10, "low flow" for Q10<Q≤Q25, "moderate flow" for Q25<Q≤Q75, "high flow" for Q75<Q≤Q90 and "storm flow" for Q>Q90.

4. Discussion

4.1. In-stream processes influence carbon and nutrient dynamics at the mesoscale

The results show that in-stream processes can explain much of the temporal variability in C and nutrient concentrations at the outlet of a mesoscale catchment. The coefficient of variation for NO_3 concentration increased from 0.21 in the integrated source signal to 0.52 at the outlet of the Yvel catchment. It also increased from 0.35 to 0.65 and from 0.32 to 0.41 for TP and DOC concentrations, respectively. In-stream processes influenced DOC variations

less than NO_3 and TP variations. For SRP, the coefficient of variation decreased from 0.45 to 0.36, showing that the river network can also buffer concentration dynamics.

This observation contrasts with other studies of headwater and mesoscale catchments, in which variations were attributed exclusively to the mixing of water from different compartments (e.g. Abbott et al., 2018; Zhi et al., 2019). In the present study, it seems unlikely that the alterations observed between the source and outlet signals could have been due to mixing with another source of water. The only other possible source of water would be deep groundwater, which can feed rivers downstream and whose proportion can increase in summer (Tiwari et al., 2014). To support this hypothesis, however, the chemical composition of deep groundwater would need to (1) vary over time, because alterations of NO_3, TP and DOC signals were not synchronous, and (2) be poor in NO_3 and TP but rich in DOC, to be able to account for the differences between modelled source and measured outlet concentrations. Low NO3 and TP concentrations match the concentrations in local deep groundwater, but not the necessary high DOC concentrations, as groundwater both in the region (Aubert et al., 2013) and elsewhere (Dick et al., 2014) are generally poor in DOC. In addition, the neighbouring research catchment of Kervidy-Naizin (5km²) lying 50 km west of the Yvel catchment, with its similar size, soil-climate and land-use conditions to those of the subcatchments monitored in the present study, has a closed water balance (Fovet et al., 2018).

Two main processes may be responsible for apparent NO_3 retention in the river network at low flow: autotrophic primary production and heterotrophic denitrification at the water/sediment interface. For macrophytes, NO_3 retention is temporary because they decompose in autumn and release dissolved inorganic N (DIN) (Riis et al., 2019). For suspended algae, apparent NO_3 retention actually represents transformation into organic N, which will transit through the river network. It is generally accepted that heterotrophic denitrification removes more NO_3 than assimilatory uptake (Reisinger et al., 2015), but the data available in the Yvel catchment do not allow to distinguish the relative influence of

dissimilatory denitrification and assimilatory uptake to be quantified. Future studies based on analysing N isotopes and/or biological parameters can be performed to clarify the relative influence of the two processes.

In-stream alteration of P dynamics may be controlled by assimilatory uptake, adsorption/desorption (of dissolved P) and sedimentation/remobilisation (of particulate P). At the outlet, particulate P represents up to 70% of TP at high flow (Fig. 6S, Supplementary material). Particulate P is stored temporarily at low flow or during flow recession as sediments on the riverbed. This P stock may be remobilised as particulate P during subsequent high-flow events or released as SRP due to processes such as reductive dissolution of P-bearing iron oxides in anoxic sediments (Kreiling et al., 2019a). TP alteration in the Yvel river network varied greatly over time, with no period of conservative transport (Fig. 7D). P load apportionment models often assume conservative and immediate transport of point-source inputs to the outlet (e.g. (Grene et al., 2011)). However, our results show that river networks may influence P dynamics greatly, due to high P retention during low flow and P remobilisation during high flow. These mechanisms of temporary retention and remobilisation may cause load apportionment models to underestimate P point-source loads, as also highlighted by Jarvie et al. (2012).

DOC alteration in river network modelling studies often show apparent retention (Wollheim et al., 2015; Mineau et al., 2016; Czuba et al., 2018), although some studies show apparent production in forested (Finlay et al., 2011) and agricultural catchments (Fovet et al., 2020). Our results reveal no DOC retention, but instead show conservative DOC transport or DOC production, regardless of temperature or flow. Apparent retention can be assumed to be caused by mineralisation of DOC by photodegradation or heterotrophic respiration. Apparent production can be due to release of soluble C from living or dead vegetation due to autotrophic processing of riverbed sediments C by microorganisms. DOC can also be released by diffusion or remobilisation and desorption of sediments (Fovet et al., 2020). The apparent production calculated for very high flow could be due to desorption, as it is usually

synchronous with TP production (Fig. 8B and 8C), while apparent production at very low flow could be due to a combination of several biotic processes.

4.2. Hydrological control of river network alterations

Our results show that discharge was the primary control of apparent retention and remobilisation processes in the river network of the Yvel catchment. Neither temperature nor input concentration correlated with observed river network alteration rates (Figs. 4S and 5S, Supplementary material), unlike results from previous studies of nutrient uptake rate in a variety of ecological settings (Mulholland et al., 2008; Wollheim et al., 2008). Discharge is a proxy of residence time in the hydrographic network: the lower the discharge, the longer the residence time and the higher the alteration rate (apparent retention of NO_3 and TP, apparent production of DOC). Our observations are thus in line with those of other studies that indicate that residence time in the river network is the main control of in-stream processes (Zarnetske et al., 2011; Abbott et al., 2016; Maranger et al., 2018).

The Yvel catchment has a particularly pronounced low-flow season for the region, due to its schist-dominated geology. Catchments with less pronounced low flow, such as those overlying granite, would arguably have lower river network alteration rates because of shorter residence times in the river network at low flow. Previous studies that compared schist and granite catchments in Brittany have indeed shown greater seasonal variation in "flashy" schist catchments than in "damped" granite catchments, which could be related in part to different in-stream alteration rates (Gascuel-Odoux et al., 2010; Abbott et al., 2018; Dupas et al., 2018). Our empirical results also confirm results of analytical modelling studies that show that in-stream processes have more influence in "flashy" streams than in "damped" streams (Basu et al., 2011).

The strong A-Q relationships observed in this study may help interpret the C-Q relationship observed in mesoscale catchments, namely the relative influence of hillslope and in-stream processes (Meybeck and Moatar, 2012). In-stream processes can both amplify and dampen the C-Q slopes observed in the headwater and point-source signals. In the Yvel catchment,

the NO_3 input signal was nearly flat, and most seasonal NO_3 dynamics at the outlet were explained by in-stream retention, especially below median discharge. This change in behaviour at median discharge supports the observation of (Moatar et al., 2017) that C-Q slopes may differ on each side of median discharge. Conversely, for TP, in-stream processes appear to dampen the expected seasonal increase in concentration due to a lack of dilution of point sources. However, remobilisation of riverbed sediments amplified the positive A-Q relationship for the TP already observed in the input signal at high flow. The A-Q pattern for DOC is not as clear as those for NO_3 and TP, and the alterations are generally weaker. Nevertheless, it reveals that the increase in DOC concentrations at low flow is an in-stream process and that the flushing pattern in the headwater catchments at high flow is either transferred conservatively or amplified. Overall, in-stream processes determined the outlet C-Q pattern of NO_3 almost entirely, influenced considerably that of TP and had little influence on that of DOC.

4.3. Impacts on annual mass balances

When applying A-Q relationships to the 2009-2018 discharge data, we estimated annual NO_3 retention to range from 9-14%, annual DOC production to range from 16-49% and annual TP production to range from 41-174%. However, we also observed outliers to the A-Q relationship during storm events, especially for TP and DOC (Figs. 7D and 7F), which could have led to high uncertainties in their annual retention/production rates.

Despite high in-stream retention at low flow, our estimate of annual NO_3 mass retention from 2009-2018 was relatively low (9-14%). This estimate of apparent removal is of the same magnitude as that of Wollheim et al. (2008), who observed total DIN removal of 15-33% in a 400 km² suburban catchment with a much lower N source concentration: 1.5 mg $DIN.L^{-1}$ vs. 4.5-9.5 mg $N.L^{-1}$ in the Yvel catchment (Fig. 6A). Seitzinger et al. (2002) observed total N removal of 37-76% for 16 catchments with a Strahler order of 5-8 and size of 475-70,189 km². For the smaller catchments studied by Seitzinger et al. (2002), total removal was 37% for an estimated TN source load of 644 $kg.km^{-2}.y^{-1}$, which is smaller than to that our study,

with an estimated NO_3 source load of 1710 kg.km^{-2}.y^{-1}. Relative removal was thus about one-third as high in our study, but absolute removal was similar (154-209 vs. 238 kg N.km^{-2}.y^{-1} for NO_3 and TN, respectively). The somewhat lower in-stream N retention rate estimated in the Yvel catchment compared to that in the literature may thus be due to the high N inputs in catchments in Brittany and is in line with the recently developed river network saturation concept (Wollheim et al., 2018).

The A-Q relationship had a moderate influence on DOC loads at the outlet, with total annual apparent production from 2009-2018 of 16-49% (median 25%). This implies that 67-84% (median 80%) of DOC found at the outlet enters the river network in the headwaters. This observation contrasts with those of previous studies in the literature, which usually observe DOC degradation in river networks (Mineau et al., 2016; Czuba et al., 2018). The main reason for this particular behaviour may be that streams that drain agricultural catchments have different organic matter composition than those that drain forested or peatland catchments, as suggested recently by Fovet et al. (2020). It is important to note, however, that this result is uncertain, because the flushing pattern of the A-Q relationship above median Q was statistically weak (R^2 = 0.10, p = 0.20) but had a disproportionally large influence on annual mass balance.

For TP, the A-Q model estimated high annual apparent production that ranged from 42-174% from 2009-2018. According to Westphal et al. (2019), we should have expected instead a balanced long-term mass balance for TP. Like for DOC, this estimate must be considered with caution because most annual TP load can transit in a few storm events each year (Cassidy and Jordan, 2011), and outliers to the fitted A-Q model often corresponded to storm events (Fig. 7D). Because increase in concentration during storm events is spikier in headwaters than at the outlet, our sampling design was more likely to capture storm events at the outlet than in the headwaters, which may have led to overestimation of in-stream TP apparent production. As a consequence, the uncertainty in our mass-balance calculation for each date increases during unstable hydrological conditions. This issue is reflected in our A-

Q plots, where dates identified as unstable diverge from the regression line for DOC and TP (Figure 7 D and F). To address this issue, future research would need to include high-resolution monitoring equipment (Wollheim et al., 2017; Jarvie et al., 2018), Lagrangian sampling (Hensley et al., 2019; Ritz and Fischer, 2019) or time-integrated monitoring techniques (Zabiegala et al., 2010; Knutsson et al., 2013). It is also possible that our assumption of constant delivery from point sources, which we verified on two sampling dates upstream and downstream of each of the seven WWTPs in the catchment, did not capture episodic TP release from some of the WWTPs during storm events. These episodic releases can be confused with TP apparent production in the river-network. In order to overcome this limitation in future research, we suggest performing the WWTP monitoring on the same dates as the subcatchment synoptic sampling. Similar to the above proposed methods of subcatchment monitoring, an interesting but costly development would be to implement high-resolution or time-integrated monitoring techniques. Overall, applying the A-Q relationship to infer annual retention/production is likely to provide reliable results for solutes that are exported mainly during baseflow periods, such as NO_3, but not for DOC and TP, which are exported mainly during storm events (Cassidy and Jordan, 2011; Humbert et al., 2015).

4.4. Consequences for nutrient ratios

In-stream processes influence nutrient concentration dynamics much more (sections 4.1 and 4.2) than they influence annual fluxes (section 4.3). At low flow, while DOC concentration increases at the outlet due to in-stream production processes, TP and SRP concentrations remain stable as sedimentation and adsorption processes dampen the point-source loads, and NO_3 concentration decreases sharply because of the development of removal/retention processes in the river network (section 4.2).

These dynamics have a strong influence on nutrient ratios at the outlet of the mesoscale catchment studied and thus at the inlet of a sensitive receiving water body (section 2.1). During the low-flow period, the C:N ratio at the outlet of the study site, calculated as the molar ratio of (DIC+DOC)/NO_3, increased strongly up to 180C:1N (Fig. 7S, Supplementary

material). Given the Redfield ratio (106C:16N), such a high ratio suggests N limitation for autotrophic production at the mesoscale outlet when discharge is <100 $L.s^{-1}$. Regarding the N:P ratio, calculated as the molar ratio of $TDP:NO_3$, we observed P limitation in the source signal for all discharge conditions (N:P ratio >147N:1P; Fig. 8S, Supplementary material). When discharge was <100 $L.s^{-1}$ at the outlet, the N:P ratio was <16N:1N on two dates, 16N:1P-32N:1P on two dates and >32N:1P on three dates. These ratios suggest that N can be a limiting or co-limiting nutrient for autotrophic production when it enters a sensitive freshwater body such as the Lac au Duc. This P limitation due to apparent N retention was also observed in other river networks (e.g. Kreiling et al. (2019b). When N is the limiting nutrient, certain cyanobacteria can fix atmospheric N and then be favoured by the subsequent conditions. N limitation in the water column and the ability of cyanobacteria to fix atmospheric N suggests they can gain a competitive advantage over other algae and that their biomass can be sensitive to P loads. Hence, in-stream processes in rivers that feed lakes can contribute to cyanobacterial blooms in lakes by creating N-limiting conditions during ecologically sensitive periods, a process rarely acknowledged by water quality managers.

Conclusion

An original combination of synoptic sampling campaigns, spatial stochastic modelling and mass-balance calculations allowed us to show that in-stream processes, even at the mesoscale, alter C-N-P concentrations strongly, but differently, depending on discharge, and thus the C and nutrient ratios at the outlet of the river network. At this scale, however, annual loads are influenced much less than infra-annual concentration dynamics, because biogeochemical transformations increase during low flow, while loads increase during high flow.

The results were observed for a flashy and highly eutrophic mesoscale catchment: river network alterations are probably weaker in catchments with a more buffered hydrology. Such flashy catchments can retain large amounts of nutrients during the low-flow period. The increase in the frequency and intensity of droughts in temperate regions predicted by climate projections would enhance in-stream dynamics at the mesoscale. The A-Q relationships observed in the present study are simple proxies to assess river network alterations of concentration dynamics in mesoscale catchments and could be extrapolated to a non-stationary climate.

Acknowledgement

The authors were supported by the Interreg project Channel Payments for Ecosystem Services, funded through the European Regional Development Fund (ERDF).

References

Abbott BW, Baranov V, Mendoza-Lera C, Nikolakopoulou M, Harjung A, Kolbe T, et al. Using multi-tracer inference to move beyond single-catchment ecohydrology. Earth-Science Reviews 2016; 160: 19-42. doi: 10.1016/j.earscirev.2016.06.014

Abbott BW, Bishop K, Zarnetske JP, Minaudo C, Chapin FS, Krause S, et al. Human domination of the global water cycle absent from depictions and perceptions. Nature Geoscience 2019; 12: 533-540. doi: 10.1038/s41561-019-0374-y

Abbott BW, Moatar F, Gauthier O, Fovet O, Antoine V, Ragueneau O. Trends and seasonality of river nutrients in agricultural catchments: 18years of weekly citizen science in France. Science of the Total Environment 2018; 624: 845-858. doi: 10.1016/j.scitotenv.2017.12.176

Aguilera R, Marcé R, Sabater S. Modeling nutrient retention at the watershed scale: Does small stream research apply to the whole river network? Journal of Geophysical Research: Biogeosciences 2013; 118: 728-740. doi: 10.1002/jgrg.20062

Aubert AH, Gascuel-Odoux C, Gruau G, Akkal N, Faucheux M, Fauvel Y, et al. Solute transport dynamics in small, shallow groundwater-dominated agricultural catchments: insights from a high-frequency, multisolute 10 yr-long monitoring study. Hydrology and Earth System Sciences 2013; 17: 1379-1391. doi: 10.5194/hess-17-1379-2013

Basu NB, Rao PSC, Thompson SE, Loukinova NV, Donner SD, Ye S, et al. Spatiotemporal averaging of in-stream solute removal dynamics. Water Resources Research 2011; 47: 13. doi: 10.1029/2010wr010196

Bol R, Gruau G, Mellander P-E, Dupas R, Bechmann M, Skarbøvik E, et al. Challenges of Reducing Phosphorus Based Water Eutrophication in the Agricultural Landscapes of Northwest Europe. Frontiers in Marine Science 2018; 5. doi: 10.3389/fmars.2018.00276

Botter M, Burlando P, Fatichi S. Anthropogenic and catchment characteristic signatures in the water quality of Swiss rivers: a quantitative assessment. Hydrology and Earth System Sciences 2019; 23: 1885-1904. doi: 10.5194/hess-23-1885-2019

Breiman L. Random Forests. Machine Learning 2001; 45: 5-32. doi: 10.1023/a:1010933404324

Burns DA, Pellerin BA, Miller MP, Capel PD, Tesoriero AJ, Duncan JM. Monitoring the riverine pulse: Applying high-frequency nitrate data to advance integrative understanding of biogeochemical and hydrological processes. Wiley Interdisciplinary Reviews: Water 2019: e1348. doi: 10.1002/wat2.1348

Cassidy R, Jordan P. Limitations of instantaneous water quality sampling in surface-water catchments: Comparison with near-continuous phosphorus time-series data. Journal of Hydrology 2011; 405: 182-193. doi: 10.1016/j.jhydrol.2011.05.020

Czuba JA, Hansen AT, Foufoula-Georgiou E, Finlay JC. Contextualizing Wetlands Within a River Network to Assess Nitrate Removal and Inform Watershed Management. Water Resources Research 2018; 54: 1312-1337. doi: 10.1002/2017WR021859

Dick JJ, Tetzlaff D, Birkel C, Soulsby C. Modelling landscape controls on dissolved organic carbon sources and fluxes to streams. Biogeochemistry 2014; 122: 361-374. doi: 10.1007/s10533-014-0046-3

Dupas R, Delmas M, Dorioz J-M, Garnier J, Moatar F, Gascuel-Odoux C. Assessing the impact of agricultural pressures on N and P loads and eutrophication risk. Ecological Indicators 2015; 48: 396-407. doi: 10.1016/j.ecolind.2014.08.007

Dupas R, Jomaa S, Musolff A, Borchardt D, Rode M. Disentangling the influence of hydroclimatic patterns and agricultural management on river nitrate dynamics from sub-hourly to decadal time scales. Sci Total Environ 2016; 571: 791-800. doi: 10.1016/j.scitotenv.2016.07.053

Dupas R, Minaudo C, Gruau G, Ruiz L, Gascuel-Odoux C. Multidecadal Trajectory of Riverine Nitrogen and Phosphorus Dynamics in Rural Catchments. Water Resources Research 2018. doi: 10.1029/2018wr022905

Ensign SH, Doyle MW. Nutrient spiraling in streams and river networks. Journal of Geophysical Research: Biogeosciences 2006; 111. doi: 10.1029/2005jg000114

Finlay JC, Hood JM, Limm MP, Power ME, Schade JD, Welter JR. Light-mediated thresholds in stream-water nutrient composition in a river network. Ecology 2011; 92: 140-150. doi: 10.1890/09-2243.1

Fovet O, Cooper DM, Jones DL, Jones TG, Evans CD. Dynamics of dissolved organic matter in headwaters: comparison of headwater streams with contrasting DOM and nutrient composition. Aquatic Sciences 2020; 82. doi: 10.1007/s00027-020-0704-6

Fovet O, Ruiz L, Gruau G, Akkal N, Aquilina L, Busnot S, et al. AgrHyS: An Observatory of Response Times in Agro-Hydro Systems. Vadose Zone Journal 2018; 17: 0. doi: 10.2136/vzj2018.04.0066

Fuka D, Walter M, Archibald J, Steenhuis T, Easton Z. EcoHydRology: A Community Modeling Foundation for Eco-Hydrology, 2018.

Galloway JN, Aber JD, Erisman JW, Seitzinger SP, Howarth RW, Cowling EB, et al. The Nitrogen Cascade. BioScience 2003; 53: 341. doi: 10.1641/0006-3568(2003)053[0341:tnc]2.0.co;2

Garnier J, Ramarson A, Billen G, Thery S, Thiery D, Thieu V, et al. Nutrient inputs and hydrology together determine biogeochemical status of the Loire River (France): Current situation and possible future scenarios. Science of the Total Environment 2018; 637: 609-624. doi: 10.1016/j.scitotenv.2018.05.045

Gascuel-Odoux C, Aurousseau P, Durand P, Ruiz L, Molenat J. The role of climate on inter-annual variation in stream nitrate fluxes and concentrations. Science of the Total Environment 2010; 408: 5657-66. doi: 10.1016/j.scitotenv.2009.05.003

Gascuel-Odoux C, Fovet O, Gruau G, Ruiz L, Merot P. Evolution of scientific questions over 50 years in the Kervidy-Naizin catchment: from catchment hydrology to integrated studies of biogeochemical cycles and agroecosystems in a rural landscape. Cuadernos de Investigación Geográfica 2018; 44: 535. doi: 10.18172/cig.3383

Greene S, Taylor D, McElarney YR, Foy RH, Jordan P. An evaluation of catchment-scale phosphorus mitigation using load apportionment modelling. Sci Total Environ 2011; 409: 2211-21. doi: 10.1016/j.scitotenv.2011.02.016

Hensley RT, Kirk L, Spangler M, Gooseff MN, Cohen MJ. Flow Extremes as Spatiotemporal Control Points on River Solute Fluxes and Metabolism. Journal of Geophysical Research: Biogeosciences 2019; 124: 537-555. doi: 10.1029/2018jg004738

Humbert G, Jaffrezic A, Fovet O, Gruau G, Durand P. Dry-season length and runoff control annual variability in stream DOC dynamics in a small, shallow groundwater-dominated agricultural watershed. Water Resources Research 2015; 51: 7860-7877. doi: 10.1002/2015wr017336

IGN. RGE ALTI, Version 2.0, https://geoservices.ign.fr/ressources_documentaires/Espace_documentaire/MODELES_3D/RGE_ALTI/DC_RGEALTI_2-0.pdf, 2018, pp. 38.

Inglada J, Vincent A, Arias M, Tardy B, Morin D, Rodes I. Operational High Resolution Land Cover Map Production at the Country Scale Using Satellite Image Time Series. Remote Sensing 2017; 9: 95. doi: 10.3390/rs9010095

INSEE. Données carroyées FILOSOFI, https://www.insee.fr/f /statistiques/2520034, 2015.

Jarvie HP, Sharpley AN, Kresse T, Hays PD, Williams RJ, King SM, et al. Coupling High-Frequency Stream Metabolism and Nutrient Monitoring to Explore Biogeochemical Controls on Downstream Nitrate Delivery. Environmental Science & Technology 2018; 52: 13708-13717. doi: 10.1021/acs.est.8b03074

Jarvie HP, Sharpley AN, Scott JT, Haggard BE, Bowes MJ, Massey LB. Within-river phosphorus retention: accounting for a missing piece in the watershed phosphorus puzzle. Environmental Science & Technology 2012; 46: 13284-92. doi: 10.1021/es303562y

Knutsson J, Rauch S, Morrison GM. Performance of a passive sampler for the determination of time averaged concentrations of nitrate and phosphate in water. Environmental Science: Processes & Impacts 2013; 15: 955-62. doi: 10.1039/c3em00038a

Kreiling RM, Thoms MC, Bartsch LA, Richardson WB, Christensen VG. Complex Response of Sediment Phosphorus to Land Use and Management Within a River Network. Journal of Geophysical Research: Biogeosciences 2019a; 124: 1764-1780. doi: 10.1029/2019jg005171

Kreiling RM, Richardson WB, Bartsch LA, Thoms MC, Christensen VG. Denitrification in the river network of a mixed land use watershed: unpacking the complexities. Biogeochemistry 2019b; 143: 327-346. doi: 10.1007/s10533-019-00565-6

Le Moal M, Gascuel-Odoux C, Menesguen A, Souchon Y, Etrillard C, Levain A, et al. Eutrophication: A new wine in an old bottle? Science of the Total Environment 2018; 651: 1-11. doi: 10.1016/j.scitotenv.2018.09.139

Lê S, Josse J, Husson F. FactoMineR: An R Package for Multivariate Analysis. Journal of Statistical Software 2008; 25. doi: 10.18637/jss.v025.i01

Liaw A, Wiener M. Classification and Regression by randomForest. R News 2002; 2: 18-22

Maranger R, Jones SE, Cotner JB. Stoichiometry of carbon, nitrogen, and phosphorus through the freshwater pipe. Limnology and Oceanography Letters 2018; 3: 89-101. doi: 10.1002/lol2.10080

Meybeck M, Moatar F. Daily variability of river concentrations and fluxes: indicators based on the segmentation of the rating curve. Hydrological Processes 2012; 26: 1188-1207. doi: 10.1002/hyp.8211

Minaudo C, Dupas R, Gascuel-Odoux C, Roubeix V, Danis PA, Moatar F. Seasonal and event-based concentration-discharge relationships to identify catchment controls on nutrient export regimes. Advances in Water Resources 2019; 131: 11. doi: 10.1016/j.advwatres.2019.103379

Mineau MM, Wollheim WM, Buffam I, Findlay SEG, Hall RO, Hotchkiss ER, et al. Dissolved organic carbon uptake in streams: A review and assessment of reach-scale measurements. Journal of Geophysical Research-Biogeosciences 2016; 121: 2019-2029. doi: 10.1002/2015jg003204

Mineau MM, Wollheim WM, Stewart RJ. An index to characterize the spatial distribution of land use within watersheds and implications for river network nutrient removal and export. Geophysical Research Letters 2015; 42: 6688-6695. doi: 10.1002/2015gl064965

Moatar F, Abbott BW, Minaudo C, Curie F, Pinay G. Elemental properties, hydrology, and biology interact to shape concentration-discharge curves for carbon, nutrients, sediment, and major ions. Water Resources Research 2017; 53: 1270-1287. doi: 10.1002/2016wr019635

Molénat J, Durand P, Gascuel-Odoux C, Davy P, Gruau G. Mechanisms of Nitrate Transfer from Soil to Stream in an Agricultural Watershed of French Brittany. Water, Air, and Soil Pollution 2002; 133: 161-183. doi: 10.1023/A:1012903626192

Mulholland PJ, Helton AM, Poole GC, Hall RO, Hamilton SK, Peterson BJ, et al. Stream denitrification across biomes and its response to anthropogenic nitrate loading. Nature 2008; 452: 202-5. doi: 10.1038/nature06686

Murphy J, Riley JP. A modified single solution method for the determination of phosphate in natural waters. Analytica chimica acta 1962; 27: 31-36

Musolff A, Fleckenstein JH, Rao PSC, Jawitz JW. Emergent archetype patterns of coupled hydrologic and biogeochemical responses in catchments. Geophysical Research Letters 2017; 44: 4143-4151. doi: 10.1002/2017gl072630

Musolff A, Schmidt C, Rode M, Lischeid G, Weise SM, Fleckenstein JH. Groundwater head controls nitrate export from an agricultural lowland catchment. Advances in Water Resources 2016; 96: 95-107. doi: 10.1016/j.advwatres.2016.07.003

Nathan RJ, McMahon TA. Evaluation of Automated Techniques for Base Flow and Recession Analyses. Water Resources Research 1990; 26: 1465-1473

ODEM. Apports de phosphore et prolifération de cyanobactéries dans le Lac au Duc (Morbihan), 2012, pp. 191.

R Core Team. R: A Language and Environment for Statistical Computing. R Foundation for Statistical Computing, Vienna, Austria, 2019.

Reisinger AJ, Tank JL, Rosi-Marshall EJ, Hall RO, Baker MA. The varying role of water column nutrient uptake along river continua in contrasting landscapes. Biogeochemistry 2015; 125: 115-131. doi: 10.1007/s10533-015-0118-z

Richards S, Withers PJA, Paterson E, McRoberts CW, Stutter M. Potential tracers for tracking septic tank effluent discharges in watercourses. Environmental Pollution 2017; 228: 245-255. doi: 10.1016/j.envpol.2017.05.044

Riis T, Tank JL, Reisinger AJ, Aubenau A, Roche KR, Levi PS, et al. Riverine macrophytes control seasonal nutrient uptake via both physical and biological pathways. Freshwater Biology 2019. doi: 10.1111/fwb.13412

Ritz S, Fischer H. A Mass Balance of Nitrogen in a Large Lowland River (Elbe, Germany). Water 2019; 11: 2383. doi: 10.3390/w11112383

Seitzinger SP, Styles RV, Boyer EW, Alexander RB, Billen G, Howarth RW, et al. Nitrogen retention in rivers: model development and application to watersheds in the northeastern U.S.A. Biogeochemistry 2002; 57: 199-237. doi: 10.1023/a:1015745629794

Steffen W, Richardson K, Rockstrom J, Cornell SE, Fetzer I, Bennett EM, et al. Sustainability. Planetary boundaries: guiding human development on a changing planet. Science 2015; 347: 1259855. doi: 10.1126/science.1259855

Tank JL, Rosi-Marshall EJ, Baker MA, Hall RO. Are rivers just big streams? A pulse method to quantify nitrogen demand in a large river. Ecology 2008; 89: 2935-2945. doi: 10.1890/07-1315.1

Tiwari T, Laudon H, Beven K, Ågren AM. Downstream changes in DOC: Inferring contributions in the face of model uncertainties. Water Resources Research 2014; 50: 514-525. doi: 10.1002/2013wr014275

Van Drecht G, Bouwman AF, Knoop JM, Beusen AHW, Meinardi CR. Global modeling of the fate of nitrogen from point and nonpoint sources in soils, groundwater, and surface water. Global Biogeochemical Cycles 2003; 17: 20. doi: 10.1029/2003gb002060

Water Framework Directive. 60/EC Directive of the European Parliament and the Council of October 2000 establishing a framework for Community action in the field of water policy. Official Journal of the European Communities from 2000; 22: 327

Westphal K, Graeber D, Musolff A, Fang Y, Jawitz JW, Borchardt D. Multi-decadal trajectories of phosphorus loading, export, and instream retention along a catchment gradient. Science of the Total Environment 2019; 667: 769-779. doi: 10.1016/j.scitotenv.2019.02.428

Williams M, Kumar A, Ort C, Lawrence MG, Hambly A, Khan SJ, et al. The use of multiple tracers for tracking wastewater discharges in freshwater systems. Environmental Monitoring and Assessment 2013; 185: 9321-32. doi: 10.1007/s10661-013-3254-8

Wollheim WM, Bernal S, Burns DA, Czuba JA, Driscoll CT, Hansen AT, et al. River network saturation concept: factors influencing the balance of biogeochemical supply and demand of river networks. Biogeochemistry 2018; 141: 503-521. doi: 10.1007/s10533-018-0488-0

Wollheim WM, Mulukutla GK, Cook C, Carey RO. Aquatic Nitrate Retention at River Network Scales Across Flow Conditions Determined Using Nested In Situ Sensors. Water Resources Research 2017; 53: 9740-9756. doi: 10.1002/2017wr020644

Wollheim WM, Peterson BJ, Thomas SM, Hopkinson CH, Vorosmarty CJ. Dynamics of N removal over annual time periods in a suburban river network. Journal of Geophysical Research-Biogeosciences 2008; 113: 17. doi: 10.1029/2007jg000660

Wollheim WM, Stewart RJ, Aiken GR, Butler KD, Morse NB, Salisbury J. Removal of terrestrial DOC in aquatic ecosystems of a temperate river network. Geophysical Research Letters 2015; 42: 6671-6679. doi: 10.1002/2015gl064647

Ye S, Reisinger AJ, Tank JL, Baker MA, Hall RO, Rosi EJ, et al. Scaling Dissolved Nutrient Removal in River Networks: A Comparative Modeling Investigation. Water Resources Research 2017; 53: 9623-9641. doi: 10.1002/2015gl064647

Zabiegala B, Kot-Wasik A, Urbanowicz M, Namiesnik J. Passive sampling as a tool for obtaining reliable analytical information in environmental quality monitoring. Analytical and Bioanalytical Chemistry 2010; 396: 273-96. doi: 10.1007/s00216-009-3244-4

Zarnetske JP, Haggerty R, Wondzell SM, Baker MA. Dynamics of nitrate production and removal as a function of residence time in the hyporheic zone. Journal of Geophysical Research 2011; 116. doi: 10.1029/2010jg001356

Zhi W, Li L, Dong W, Brown W, Kaye J, Steefel C, et al. Distinct Source Water Chemistry Shapes Contrasting Concentration-Discharge Patterns. Water Resources Research 2019. doi: 10.1029/2018wr024257

Antoine Casquin: Conceptualization, Methodology, Formal Analysis, Writing - Original Draft, Writing - Review & Editing, Visualization. **Sen Gu**: Investigation, Writing - Review & Editing. **Rémi Dupas**: Conceptualization, Writing - Review & Editing, Supervision, Funding acquisition. **Patrice Petitjean**: Investigation, Writing – Review & Editing. **Gérard Gruau**: Writing - Review & Editing, Project administration. **Patrick Durand**: Writing - Review & Editing, Supervision.

Declaration of interests

☒ The authors declare that they have no known competing financial interests or personal relationships that could have appeared to influence the work reported in this paper.

☐The authors declare the following financial interests/personal relationships which may be considered as potential competing interests:

Table 1. Estimated daily total loads (kg) of NO_3, TP, SRP, DOC and Cl for the two point-source sampling dates

Date	NO_3	TP	SRP	DOC	Cl	Flow condition
24 Sep 2018	53.2	1.97	1.62	18.8	162.8	drought
11 Dec 2018	57.1	2.00	1.25	3.3	168.7	moderate flow

Graphical abstract

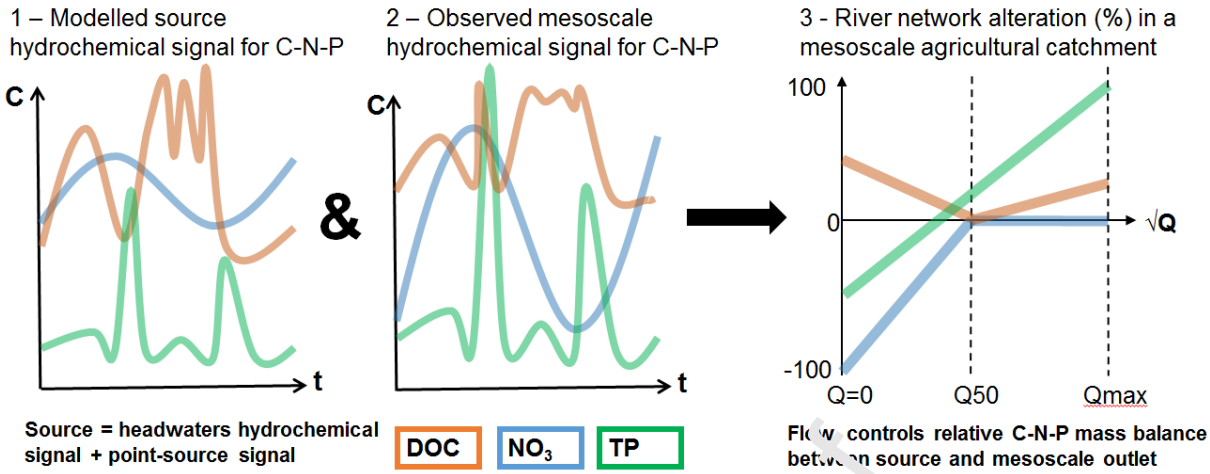

Highlights

1. Assessment of in-stream alterations of C-N-P dynamics in a mesoscale catchment
2. Repeated synoptic sampling of headwaters and stochastic landscape mixing modelling
3. In-stream processes influence C-N-P dynamics greatly but annual loads little
4. Streamflow is the key control of in-stream processes